International Journal of Chemistry; Vol. 8, No. 2; 2016
ISSN 1916-9698 E-ISSN 1916-9701
Published by Canadian Center of Science and Education

Creation of Photoactive Inorganic/Organic Interfaces Using Occlusion Electrodeposition Process of Inorganic Nanoparticles during Electropolymerization of 2,2′:5′,2″-Terthiophene

Kasem K. Kasem[1], Christopher Santuzzi[1], Nick Daanen[1], Kortany Baker[1]

[1]School of Sciences, Indiana University Kokomo, Kokomo, IN, 46904, USA

Correspondence: Kasem K. Kasem, School of Sciences, Indiana University Kokomo, Kokomo, IN, 46904, USA.

E-mail: kkasem@iuk.edu

Received: December 22, 2015 Accepted: January 5, 2016 Online Published: March 10, 2016

doi:10.5539/ijc.v8n2p1 URL: http://dx.doi.org/10.5539/ijc.v8n2p1

Abstract

Photoactive (IOI) inorganic/organic interface assemblies were prepared using an occlusion electrodeposition method. Poly-2,2′:5′,2″-Terthiophene (PTTh) were the organic thin films that occluded each of CdS, TiO_2, and Zn-doped WO_3 nanoparticles. The energy band gap structures were investigated using spectroscopic and electrochemical techniques. The obtained assemblies were investigated in aqueous solutions under both dark and illuminated conditions. The results were compared with the behavior of PTTh thin film. Oxygen played an important role in minimizing electron/hole recombination as was evident by observed very low photocurrent when oxygen was removed by nitrogen purge. Results show that PTTh/CdS gave the greatest photocurrent, followed by PTTh/Zn-WO_3 and PTTh/TiO_2.

Keywords: Photoelectrochemistry, Interface, Occlusion, Inorganic, Organic semiconductors

1. Introduction

Surface modification can create or eliminate defects and alter the energy band structure of the modified surface, consequently altering the donor /acceptor character of the modified surfaces. Some modifications require co-immobilization of several substances on the electrode surface. However, when the semiconductor's particle preparation and immobilization/deposition steps are separated, the intrinsic nature of the semiconductor particles (e.g., size, morphology, and crystal structure) are greatly altered or compromised by the deposition process itself. A search for simple and direct methods for immobilization is very important (Withers J. C et al 1961). One of the simple methods with fewer steps that can enhance intrinsic properties is occlusion. Occlusion involves immobilization of semiconductor particles in the matrix of an electrochemically synthesized substance.

Composite films containing occluded TiO_2 (Tomaszewski et al 1963, Tomaszewski et al 1969, and Hovestad A. et al 1995) or CdS (Tacconi NR de et al 1997) particles in a Ni matrix were prepared. Other metal matrices such as Ni, Cu, Ag, In (Zhou M. et al 1996) or in poly-pyrrole (Beck P. et al 1992) have been utilized for immobilizing the TiO_2 particles.

Occlusion electrodeposition of ZnO and carbon nanotubes has been reported (Haining Chen, et al 2011). Further studies (Santos, M. J. L et al 2009) show that CdS and CdS/ZnS enhance the photoelectrochemical behavior of poly-terthiophene. Poly-terthiophene was used to modify the surface of CdS nanoparticles by adsorption of the monomer on CdS particles, followed by photopolymerization of the adsorbed monomer. The modified CdS particles were studied in nanopowder form or in solid thin film composite over ITO (Kasem K. et al 2012). However the modification of CdS surface involved several separate steps (especially the photopolymerization step) that may negatively affected the intrinsic properties of the CdS/PTTh assembly.

In this paper we explored the use of the occlusion electrodeposition (OE) process for creation of an Inorganic /organic interface (IOI) between poly terthiophene (PTTh) and CdS, TiO_2, and Zn-WO_3 (Zn-doped WO_3) to judge the effects on the photoelectron-chemical behavior of the created IOI assemblies.

2. Experimental

2.1 Reagents

All the reagents were of analytical grade. All of the solutions were prepared using deionized water, unless otherwise stated.

2.2 Preparations

A- Electropolymerization of PTTh:

Polymer thin films were generated electrochemically using cyclic voltammetry (CV) technique by repetitive cycling of the FTO electrode potential at a scan rate 0.10V/s between -1.0 and 2.0 V vs Ag/AgCl in acetonitrile 1 mM of the monomer and 0.5M $LiClO_4$.

B- (Occlusion Method):

Thin films of IOI assemblies were generated electrochemically using cyclic voltammetry (CV) technique by repetitive cycling of the FTO electrode between -1.0 and 2.0V vs Ag/AgCl in acetonitrile suspension of each CdS, TiO_2 and Zn-WO_3 and 1.0 mM of the monomer and 0.5M $LiClO_4$.

C- Electrodeposition of CdS thin solid film:

CdS was prepared in two steps: first, Cd was deposited by applying -0.850V vs Ag/AgCl on a FTO working electrode in three-electrode cell containing 0.2 M $CdSO_4$ for 10 minutes, then thin solid film of Cd was deposited on a FTO and transferred to another electrochemical cell containing 2.0 M Na_2S, where it was subjected to a linear sweep volumetric between -1.0 V and 0.700 V vs Ag/AgCl at 0.01V/s scan rate. A Canarias yellow film appeared after the first scan. The generated CdS film was annealed at 150 ^oC for 60 minutes.

2.3 Instrumentation

All electrochemical experiments were carried out using a conventional three-electrode cell consisting of a Pt wire as a counter electrode, Ag/AgCl as a reference electrode, and FTO as the working electrode. Photoelectrochemical studies on thin solid films were performed on an experimental set up as illustrated in Figure 1 inset C. A BAS 100W electrochemical analyzer (Bioanalytical Co.) was used to perform the electrochemical studies. Steady state reflectance spectra were performed using Shimadzu UV-2101 PC. Irradiation was performed with a solar simulator 300 watt xenon lamp (Newport) with an IR filter.

3. Results and Discussion

3.1 Occlusion Electrodeposition of CdS, Zn-WO_3, and TiO_2 Nanoparticles in PTTh

Repetitive cycling of the FTO electrode between -1.0 and 2.0 V vs Ag/AgCl in an acetonitrile suspension of CdS nanoparticles and 1.0 mM of the monomer TTh and 0.5M $LiClO_4$ generated a homogenous thin film where CdS particles were entrapped into the film's matrix. Figure 1A shows a positive shift of the anodic peak corresponding to the polymerization of TTh monomer. Furthermore, the growth of both anodic and cathodic peaks current is indication of film build up. The coexistence of insoluble CdS nanoparticles with the monomer did not affect the electrochemical behavior of the monomer as CdS nanoparticles are electrochemically inactive under the experimental conditions. The occlusion electrodeposition of Zn-doped WO_3 was similar to that displayed in Figure 1A. On the other hand, the CV for occlusion of TiO_2 nanoparticles is displayed in Figure 1B, which again show similar behavior to that shown in Figure 1A. This is consistent with the facts that both Zn-Doped WO_3 and TiO_2 nanoparticles are electrochemically inactive under the experimental conditions.

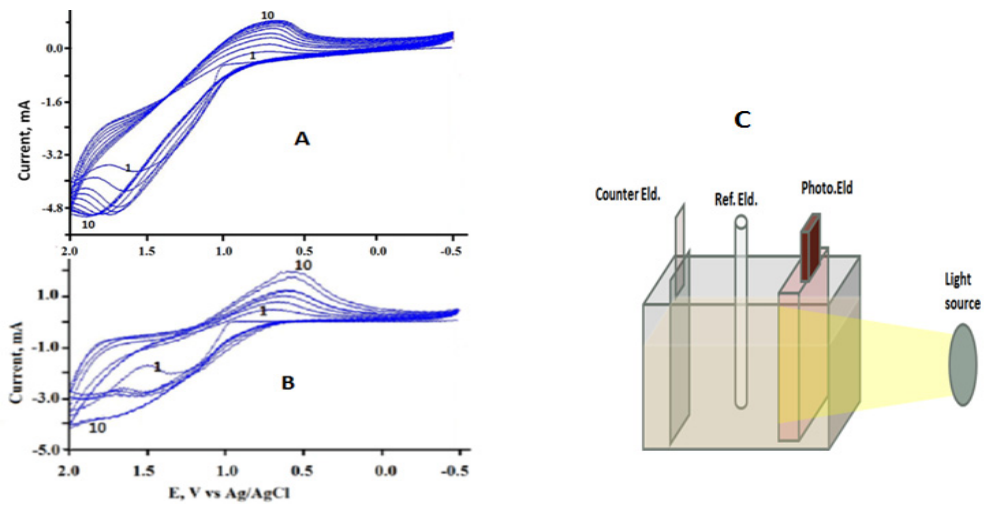

Figure 1. Electrochemical occlusion deposition of A) CdS nanoparticles, and B) TiO_2 during the polymerization of terthiophene, and C) a diagram for the Photoelectrochemical cell.

3.2 Absorption Spectra of PTTh/ Inorganic Assemblies Interfaces

Absorption spectra of the polymer PTTh and its assemblies with, CdS and Zn-Doped WO_3 were studied and the results are displayed in Figure 2. Figure 2b and 2c show the overlapping absorption peaks around the approximate band gaps of both CdS, Zn-WO_3 and PTTh. On the other hand Figure 2a shows a gradual increase of absorption that reaches maximum around TiO_2 band gap (≈3.1 eV). Furthermore, Figure 2 shows more absorption of a visible region. This can be attributed to fact that each of the occluded materials acted as absorbent beside the host polymer, resulting in the broad absorption spectra shown in Figure 2. The absorption spectra of these assemblies were subject to further analysis using Tauc equations (Robert, V. L. et al 1995, and Bhatt R. 2012). The results are listed in Table 1. The data listed in Table 1 suggest the existence of direct and indirect band gaps structures in these assemblies. The existence of a direct and indirect band gaps suggests the possibility of creating a hybrid band at the organic/inorganic interface. This would allow for band alignment (Chiatzun G. et al 2007, and Blumstengel S. et al 2008) that facilitates better charge separation and transfer processes, further leading to more efficient photochemical process.

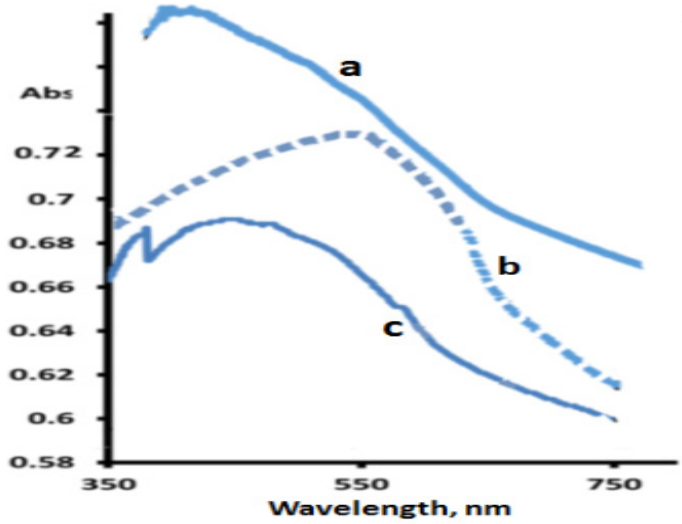

Figure 2. Absorption spectra for PTTh Occluded with a) TiO_2, b) Zn-WO_3, and c) CdS

3.3 Electrochemical Behavior of the FTO/PTTh /Inorganic Assemblies in Aqueous Phosphate Buffer

The electrochemical behaviors of FTO/PTTh/ with each of TiO_2, CdS and Zn-WO_3 CdS were investigated by cycling the potential of FTO modified with each OII assembly in the dark and light at a scan rate 0.050V/s , between -1.2 to 1.8 V vs Ag/AgCl in nitrate buffer (pH 7). Figure 3A shows that the photocurrent recorded for PTTh/TiO_2

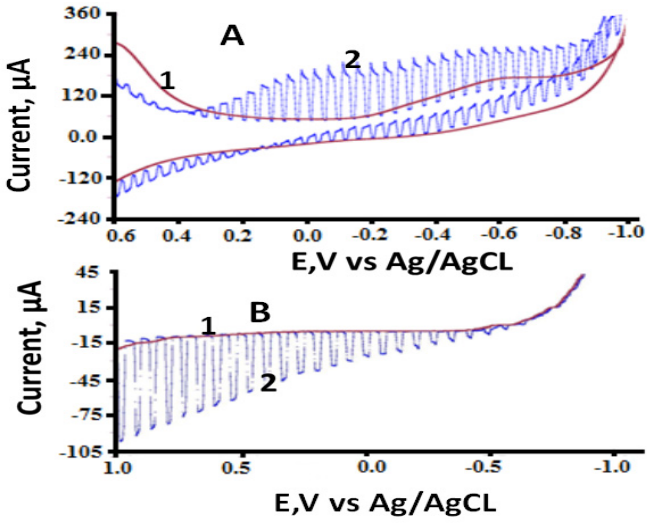

Figure 3. CV in 0.1 M KNO_3 scan rate 50 mV/S of A) FTO/PTTh/TiO_2, and B) FTO/TiO_2 1: CV Under Dark, 2):CV during illumination.

assembly is greater than that recorded under the dark conditions in both the cathodic scan between at ≈0.30 vs Ag/AgCl and the anodic scan at ≈ 0.2V vs Ag/AgCl. These potential values are more positive than that recorded for TiO_2 film only (Figure 3 B). These observations indicate that the approximate E_{fb} (flat band potential) of the assembly is at ≈ 0.2 V vs Ag/AgCl or 0.4 V vs SHE. We infer that is the value of the hybrid sub-band created upon occlusion of TiO_2 nanoparticles in PTTh. Likewise, Figures 4 and 5 show the photocurrent recorded for PTTh/ CdS (Figure 4) and PTTh/Zn-WO_3 (Figure 5) indicating that the E_{fb} in the assembly of PTTh and occluded nanoparticles are shifted to more positive potentials than in the cases of the thin films of CdS or Zn-WO_3 respectively. This again indicates the formation of hybrid sub band in these assemblies.

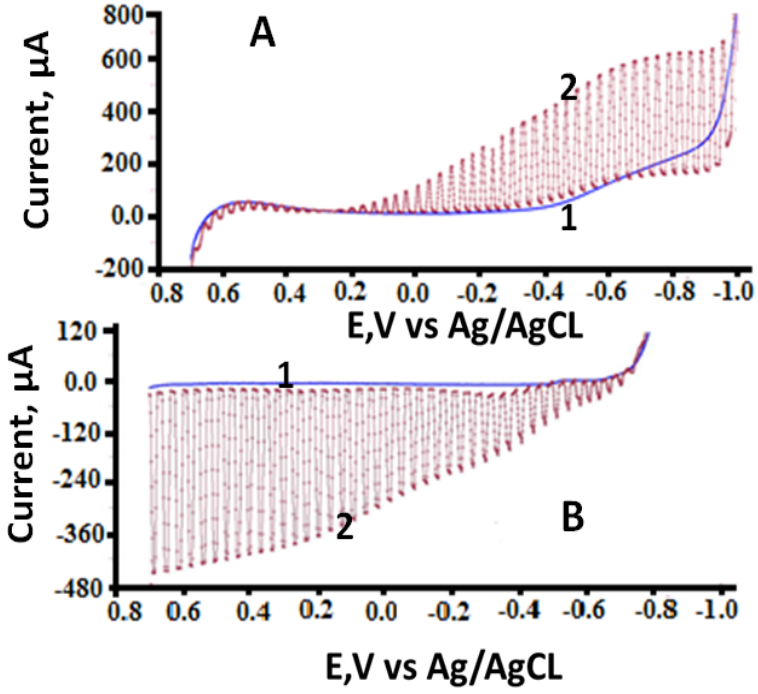

Figure 4. CV in 0.1 M KNO_3 scan rate 50 mV/S of A) FTO/PTTh/CdS, and B) FTO/CdS 1: CV in Dark, and 2: CV during illumination.

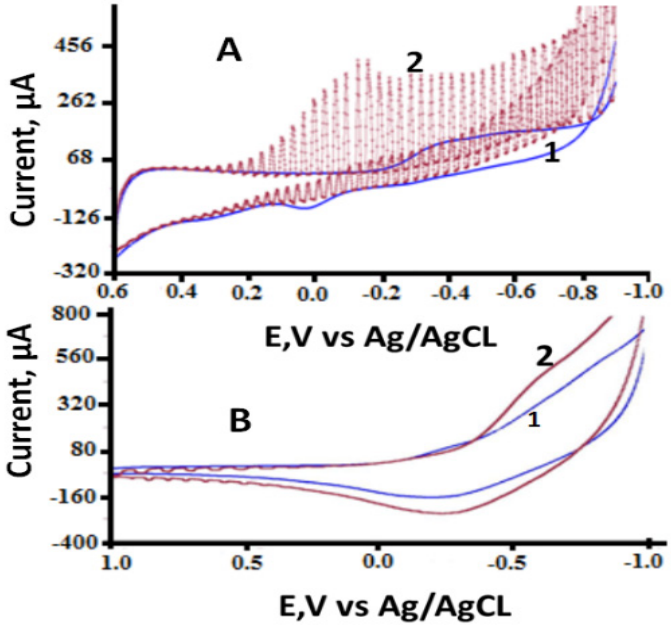

Figure 5. CV in 0.1 M KNO_3 scan rate 50 mV/S of A) FTO/PTTh/Zn-WO3, and B) FTO/Zn-WO_3 1: CV Under Dark, and 2: CV during illumination.

Because phosphate buffer is widely used in photoelectrochemical studies and the role of HPO_4^{2-} as a hole scavenger was previously studied (Abdullah M. et al 1990) , cyclic voltammetry studies was performed for the assemblies FTO/PTTh (TiO_2, CdS or Zn-WO_3) in phosphate buffer. These CV were similar but not identical to those displayed in figures 3,4, and 5. (CVs are not shown) as large photocurrent was observed in during the cathodic scan between 0.2 and -1.0 V. Table 1 lists the approximate flat band potential for each of these assemblies in KNO_3 electrolyte. It can be noticed that the occlusion process causes a positive shift in the flat band potential of the inorganic semiconductor when it occluded by PTTh film. This can be attributed to the role of the PTTh in creation of a hybrid sub-band at these assemblies/electrolyte interface.

Table 1. Band gap data and flat band potential (in KNO_3) for the studies at O/I/I

Assembly	Band Gap, eV	Direct band Gap, eV	Indirect band gap, eV	E_{fb} vs Ag/AgCl	E_{fb} pot. For inorganic only
PTTh/CdS	2.45	2.32	2.770	0.180 V	-0.70 V
PTTh/TiO_2	3.1	2.5, 2.8	3.1	0.30 V	-0.60 V
PTTh/Zn-doped WO_3	2.7	2.68	2.7	0.30 V	-0.40 V

3.4 Role of Oxygen in Suppression of Hole/Electron Recombination

As the generated photocurrent is a reflection of efficient charge separation (e/h), it is important to study the photocurrent –time relationship by monitoring the photocurrent under longer illumination time at constant potential. We have chosen phosphate buffer (pH 6) to be the electrolyte to study these assemblies photocurrent-time behavior. We performed these studies in the presence and in the absence of O_2.

In the photocurrent –time study, each assembly was illuminated under constant potential which was identified by the CV under illumination studies. The assembly was subjected to periods of illumination and darkness and the generated photocurrent was recorded over time.

Figure 6 shows photocurrent-time curve generated by subjecting the FTO/PTTh/CdS assemblies to a constant potentials under illumination for a long duration. Upon illumination of FTO/PTTh/CdS assemblies (Figure 6A) in oxygenated (aired) phosphate buffer (pH 6), a sudden increase in the current followed by slow increase in the

Photocurrent, as indicated by the formation of a positively slopping plateau. When the electrolyte was deoxygenated (after N_2 purge), the illumination generated less photocurrent and exhibited a negatively sloping plateau (Figure 6B red trace) with a steady value closer to that of the dark current was recorded. Such behavior was

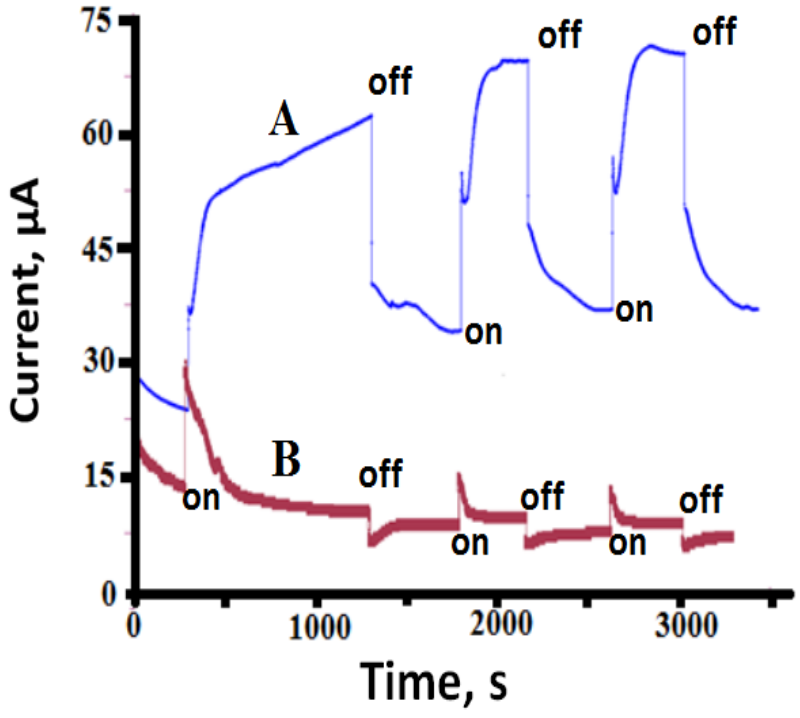

Figure 6. FTO/PTTh//CdS in Phosphate buffer at -0.600 V vs Ag/AgCl, A) In presence of O_2, and B) Deoxygenated solution in the presence of N_2.

reproducible as indicated during the illumination/dark processes. These photocurrent curves generated in presence and in absence of O_2, indicate again that O_2 plays an important role in enhancing charge separation, as demonstrated by the steady increase in photocurrent during the illumination period. In the case of FTO/PTTh/TiO_2 assembly (Figure 7A), in oxygenated phosphate buffer, a sudden increase in the current was followed by a slow increase in the photocurrent. When the electrolyte was deoxygenated (Figure 7B), the illumination generated a very low photocurrent with a slow increase in its value.

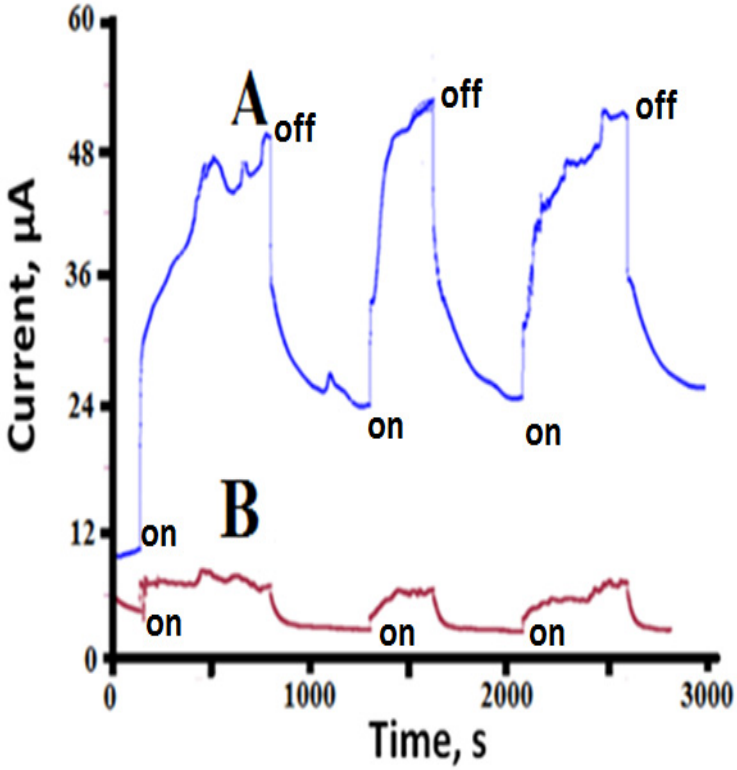

Figure 7. FTO/PTTh//TiO2 in Phosphate buffer at-0.580 V vs Ag/AgCl. A) In presence of O_2 and B) in deoxygenated solution in presence of N_2.

The behavior of FTO/PTTh/Zn-WO_3 in phosphate buffer in the presence (Figure 8A) and absence of oxygen (Figure 8B) was more or less similar to that of FTO/PTTh /CdS. It is apparent from these data that the presence of oxygen plays important role in the mechanism of charge separation and transfer at the IOI/ electrolyte interface.

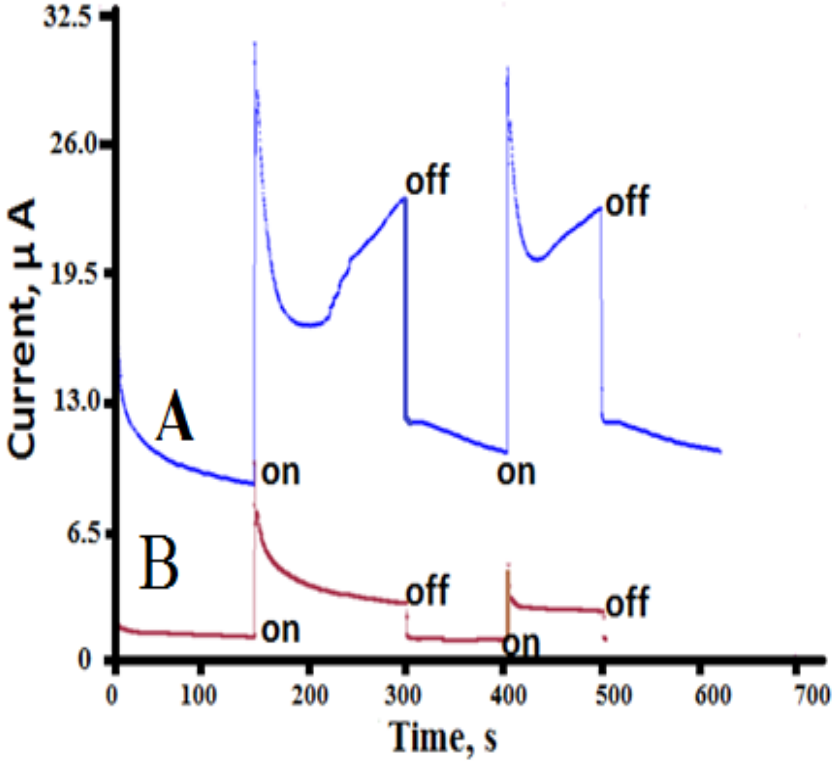

Figure 8. FTO/PTTh/Zn-WO3 in Phosphate buffer at -0.500 V vs Ag/AgCl. A) In presence of O_2 and B) in Deoxygenated solution in presence of N_2.

4. Conclusion

A photoactive inorganic /organic interface was created using occlusion electrodeposition. The reproducible photoactivities of the studied assemblies suggests that occlusion electrodeposition method is reliable and effective method for the creation of inorganic /organic interfaces. The magnitude of the photocurrent produced by each assembly is controlled by the band alignments between each assembly components. Creation of hybrid sub band between PTTh and inorganic compound was suggested as supported by previous studies (Abdullah M et al, 1990, and Chiatzun G. et al 2007).

Acknowledgment

The authors acknowledge the great contribution of Indiana University Kokomo that supported this research work.

References

Abdullah, M., Low, G. K. C., & Matthews, R. W. (1990). Effects of common inorganic anions on rates of photocatalytic oxidation of organic carbon over illuminated titanium dioxide. *J. Phys. Chem., 94*(17), 6820. http://dx.doi.org/10.1021/j100380a051

Beck, P., Dahhaus, M., & Zahedi, N. (1992). Anodic codeposition of polypyrrole and dispersed TiO_2. *Electrochem. Acta, 37*, 1265. http://dx.doi.org/10.1016/0013-4686(92)85066-T

Bhatt, R., Bhaumik, J., Ganesamoorthy, S., Karnal, A. K., Swami, M. K., Patel, H. S., & Gupta P. K. (2012). Urbach tail and bandgap analysis in near stoichiometric $LiNbO_3$ crystals. *Physics Status Solidi A*, *209*(1), 176-180. http://dx.doi.org/10.1002/pssa.201127361

Blumstengel, S., Sadofev, S., Xu, C., Puls, J., Johnson, R. L., Glowatzki, H., Koch, N., & Henneberger, F. (2008). Electronic coupling in organic-inorganic semiconductor hybrid structures with type-II energy level alignment. *Physical Review* B, *77*, 085323. http://dx.doi.org/10.1103/PhysRevB.77.085323

Chiatzun, G., Scully, S. R., & McGehee, M. D. (2007). Effects of molecular interface modification in hybrid organic-inorganic photovoltaic cells. *Journal of Applied Physics, 101*, 114503. http://dx.doi.org/10.1063/1.2737977

de Tacconi, N. R., Wenren, H., & Rajeshwar, K. (1997). Photoelectrochemical behavior of nanocomposite films of cadmium sulfide, or titanium dioxide, and nickel. *J. Electrochem. Soc*., *144*(9), 3159-3163. http://dx.doi.org/10.1149/1.1837975

Hovestad, A., & Janssen, L. J. J. (1995). Electrochemical codeposition of inert particles in a metallic matrix. *J. of Applied Electrochem., 25*, 519-527. http://dx.doi.org/10.1007/BF00573209

Chen, H. N., Li, W. P., Hou, Q., Liu, H. C., & Zhu, L. Q. (2011), A general deposition method for ZnO porous films: Occlusion electrosynthesis., *Electrochimica Acta, 56*, 9459–9466. http://dx.doi.org/10.1016/j.electacta.2011.08.037

Kasem, K., & Zia, N. (2012), Photoelectrochemical studies at CdS/PTTH nanoparticles interface. *Mat. Sciences and application*, *3*, 719-727.

Robert, V. L., Hung, C. J., Kammler, D. R., & Switzer, J. A. (1995). Optical and Electronic Transport Properties of Electrodeposited Thallium (III) Oxide Films. *J. Phys. Chem., 99*, *p* 15247.

Santos, M. J. L., Ferreira, J., Radovanovic, E., Romano, R., Alves, O. L., & Girotto, E. M. (2009). Enhancement of the photoelectrochemical response of poly (terthiophenes) by CdS(ZnS) core-shell nanoparticles. *Thin Solid Films*, *517*(18), 5523-5529. http://dx.doi.org/10.1016/j.tsf.2009.03.170

Tomaszewski, T. W., Clauss, R. J., & Brown, H. (1963). Satin nickel by codeposition of finely dispersed solids. *Tech. Proc*. *Am. Electroplater's Soc., 50*, 169.

Tomaszewski, T. W., Tomaszewski, L. C., & Brown, H. (1969). Codeposition of finely dispersed particles with metals. *Plating*, *56*, 1234 .

Withers, J. C. (1961). Protective Coatings for Refractory Metals. *Tech Rep*, *60*.

Zhou, M., Lin, W. Y., Tacconi, N. R., & Rajeshwar, K. (1996). Metal /semiconductor electrocomposite photoelectrodes. *J. Electroanal Chem*., *402*, 221-224. http://dx.doi.org/10.1016/0022-0728(95)04368-3